Precise measurement of ^{171}Yb magnetic constants for $^1S_0$–$^3P_0$ clock transition

Ang Zhang(张昂)[1,2], Congcong Tian(田聪聪)[1,2], Qiang Zhu(朱强)[1], Bing Wang(王兵)[1], Dezhi Xiong(熊德智)[1], Zhuanxian Xiong(熊转贤)[1,†], Lingxiang He(贺凌翔)[1,‡], and Baolong Lyu(吕宝龙)[1]

[1] *Key Laboratory of Atomic Frequency Standards, Innovation Academy for Precision Measurement Science and Technology, Chinese Academy of Sciences, Wuhan* 430071, *China*

[2] *University of Chinese Academy of Sciences, Beijing* 100049, *China*

(Received 12 October 2022; revised manuscript received 7 November 2022; accepted manuscript online 9 November 2022)

We present a precise measurement of ^{171}Yb magnetic constants for $^1S_0$–$^3P_0$ clock transition. The background magnetic field is firstly compensated to < 1 mGs (1 Gs $= 10^{-4}$ T) through measuring the splitting of two π transitins of ^{171}Yb clock transition at different compensation coils currents. Then, the splitting ratios of the π and σ components of ^{171}Yb clock transition at different bias magnetic fields are measured, and the first-order Zeeman coefficient is determined to be $\alpha = 199.49(5)$ Hz/Gs. The second-order Zeeman shifts at various bias magnetic fields are also measured through interleaved self-comparison in which the bias magnetic fields are modulated between high and low values. The second-order Zeeman coefficient is fitted to be $\beta = -6.09(3)$ Hz/mT^2, which is consistent with the result of NIST group.

Keywords: optical lattice clock, ytterbium atoms, Zeeman effects, magnetic constants

PACS: 06.30.Ft, 37.10.Jk, 32.70.Jz, 42.60.Da **DOI:** 10.1088/1674-1056/aca14e

1. Introduction

The frequency uncertainty and instability of the state-of-the-art optical clocks based on single-ions or neutral atoms have reached 10^{-18} level and below.[1–9] The unprecedented precision of optical atomic clocks has enabled their application in various areas, such as redefinition of the SI second,[10,11] testing general relativity,[12–14] detecting gravitational waves,[15] and searching dark matter.[16] The systematic uncertainty is one of three fundamental benchmarks (including systematic uncertainty, instability, and reproducibility) of clock performance, which is characterized by the uncertainties associated with all known effects that shift the clock frequency. One critical factor that must be accounted for is the influence of external magnetic fields on the clock frequency. The second-order Zeeman shift can reach 10^{-16} level for ^{171}Yb optical clock at a normal bias magnetic field of 1 Gs,[2] so the precise measurement of magnetic constants including first- and second-order Zeeman coefficients is essential for the systematic uncertainty evaluation of high-accuracy atomic optical clocks.

Here, we present a precise measurement of ^{171}Yb clock transition magnetic constants to evaluate ^{171}Yb optical lattice clock Zeeman shift. We firstly compensate the background magnetic field to be less than 1 mGs, which is depicted in Section 2. Then, the measurement of the first-order Zeeman coefficient α is described in Section 3. The measurement of the second-order Zeeman coefficient β is described in Section 4. Finally, we measure the vector Stark shift induced by lattice laser, which behaves like a pseudomagnetic field and is detailed in Section 5. The vector Stark shift is used to correct the splitting of π and σ transitions.

2. Background magnetic compensation

Our optical clock setup is an improved version of the previous setup.[17,18] The main improvements in the design are the application of a titanium science chamber body, a vertical optical lattice and a blackbody radiation (BBR) shield inside vacuum.[19] These improvements aim at reducing the systematic uncertainty and instability of ^{171}Yb optical lattice clock into 10^{-18} level.

The background magnetic field can lead to the deviation of quantization axis from the direction of polarization field, inducing imperfect spin polarization during states preparation. Thus, we apply three pairs of orthogonal Helmholtz coils to compensate the background magnetic field in three directions. The bias magnetic field of $B_{\rm bias}$ along the North–South direction is produced by another pair of Helmholtz coils. For an external magnetic field B felt by ^{171}Yb atoms, the splitting of two π components of $^1S_0$–$^3P_0$ clock transition Δf_B^{π} is given by

$$\Delta f_B^{\pi} \propto \alpha B = \alpha \sqrt{B_{\rm EW}^2 + B_{\rm UD}^2 + (B_{\rm NS} + B_{\rm bias})^2}, \qquad (1)$$

where α is the first-order Zeeman coefficient. The $B_{\rm EW}$, $B_{\rm UD}$, and $B_{\rm NS}$ are three orthogonal magnetic components of the

†Corresponding author. E-mail: zxxiong@apm.ac.cn
‡Corresponding author. E-mail: helx@apm.ac.cn

© 2023 Chinese Physical Society and IOP Publishing Ltd

background magnetic field along east–west, up–down, and north–south directions, respectively.

According to the Eq. (1), when the compensation coils fully cancel the background magnetic field in the east–west and up–down directions, $B_{\rm EW}$ and $B_{\rm UD}$ are equal to zero and the Δf_B^{π} has a minimal value. Therefore, we can measure the Δf_B^{π} as a function of the compensation coils current values for the east–west and up–down directions and the compensation currents corresponding to the minimum values of Δf_B^{π} can be obtained. However, the compensation current for the north–south direction can not be obtained in the same way as for the east–west and up–down directions, because the magnetic field produced by compensation coils of north–south direction and the bias magnetic field are coincident and indistinguishable. According to Eq. (1), the values of Δf_B^{π} are the same at the forward and reverse bias magnetic fields of equal magnitude, when the background magnetic field in the north–south direction can be fully canceled. Therefore, we can record the Δf_B^{π} at varied currents of north–south compensation coils for the forward and reverse bias magnetic fields, respectively. The point with equal values of Δf_B^{π} gives the current value compensating the background magnetic field in the north–south direction to zero.

The Δf_B^{π} can be measured by self-comparison, in which two interleaved servo loops are locked on one of two π transitions individually (see Fig. 1(a)). The Δf_B^{π} can be obtained from the frequency corrections difference $f_2(t) - f_1(t)$. Our 578-nm clock laser is locked to a 30-cm-long ULE optical cavity with a fraction frequency instability $\sim 3 \times 10^{-16}$ @1 s. In the clock operation, the Rabi interrogation time and the line-width of clock spectrum are 200 ms and 4 Hz, respectively. Frequency corrections are applied to an acousto–opitc-modulator (AOM1) by way of a direct digital synthesizer (DDS) and laser frequency is locked onto resonance with the clock transition. Besides, the clock laser drift calculated from frequency corrections is compensated by AOM2. When measuring the Δf_B^{π}, both the bias magnetic field coils and the background magnetic field compensation coils are applied.

Figures 1(b) and 1(c) shows the relationship between Δf_B^{π} and the current values of compensation coils for the east–west and up–down directions. The values of Δf_B^{π} can be fitted with Eq. (1) and the compensation current values can be found to be -82.9 mA and 142.6 mA at the bottom points of the fitting curves, producing fields of approximately -161.7 mGs and 278.1 mGs along the east–west and up–down directions, respectively. Figure 1(d) shows the Δf_B^{π} at varied currents of north–south compensation coils for the forward and reverse bias magnetic fields and two orange solid line are linear fitting to two sets of data. The intersection of two fitting line gives the compensation current of 13.5 mA, producing a field of approximately 26.4 mGs. After the background magnetic field compensation, we further measure the splitting of π transitions under different the bias coils currents, which can be fitted perfectly with a linear function (see Fig. 1(e)). The y-intercept of the solid fitting line is 0.35 Hz, corresponding to the residual background magnetic field < 1 mGs based on first-order Zeeman coefficient from NIST group.

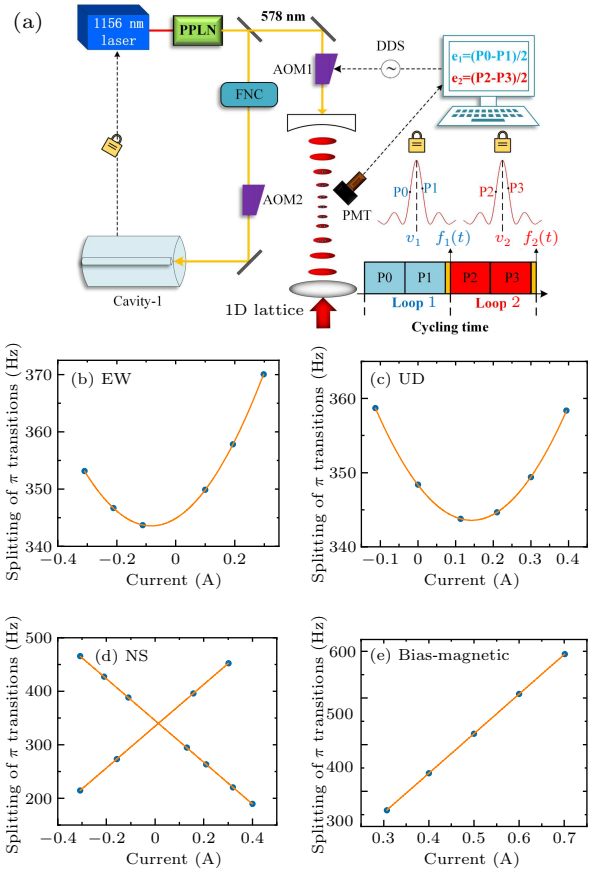


Fig. 1. Background magnetic field compensation. (a) The schematic diagram of self-comparison measurement in which two interleaved servo loops are locked on one of two π transitions individually. $f_1(t)$ and $f_2(t)$ are frequency corrections of two loops. Panels (b) and (c) show the relationships between the splitting of two π transitions Δf_B^{π} and the compensation coils currents for east–west (EW) and up–down (UD) directions. The two orange solid lines are the fitting curves with Eq. (1). (d) the Δf_B^{π} at varied currents of north–south (NS) compensation coils for the forward and reverse bias magnetic fields. Two orange solid lines are linear fitting to two sets of data. (e) Δf_B^{π} as a function of the bias coils currents. The solid line is a linear fitting to the data. The y-intercept is fitted to be 0.35 Hz.

3. First-order Zeeman coefficient

For the clock transition ($^1S_0$–$^3P_0$) of fermion ^{171}Yb (nuclear spin $I = 1/2$), it corresponds to two π transitions ($\Delta m_F = 0$) and two σ transitions ($\Delta m_F = \pm 1$) as shown in Fig. 2. In a fixed external magnetic field B_z, the energy shift of ground state $^1S_0$ is $-g_I m_F \mu_{\rm B} B_z$ which origins from nuclear spin effects only, while the exciting state $^3P_0$ experiences both nuclear spin effects and hyperfine interaction and the energy shift is $-(g_I + g_{\rm HFS}) m_F \mu_{\rm B} B_z$, and $\mu_{\rm B}$ is the Bohr magneton.[20] Thus, the linear Zeeman shifts of π and σ transitions can be written

$$\delta E_B^{\pi} = -g_{\rm HFS} m_F \mu_{\rm B} B_z,$$

$$\delta E_B^{\sigma} = -(2g_I + g_{\rm HFS}) m_F \mu_{\rm B} B_z. \tag{2}$$

Here g_I and $g_{\rm HFS}$ are the nuclear spin and hyperfine structure factor, respectively.[21] Generally, it is difficult to directly measure the magnitude of the magnetic field felt by atoms. However, the splitting of two π transitions can be precisely measured during clock operation. According to Eq. (2), if the $g_{\rm HFS}$ factor of hyperfine structure is known, the magnetic field can be determined precisely based on the splitting of two π transitions. Obviously, equation (2) can be converted into

$$\eta = \frac{\delta E_B^{\sigma}}{\delta E_B^{\pi}} = 2\frac{g_I}{g_{\rm HFS}} + 1, \tag{3}$$

where the g_I factor of ^{171}Yb has been precisely measured to be $5.3577(2) \times 10^{-4}$ as early as 1967.[22] Therefore, the hyperfine interaction $g_{\rm HFS}$ factor can be obtained by measuring the splitting ratio η of the π and σ transitions.

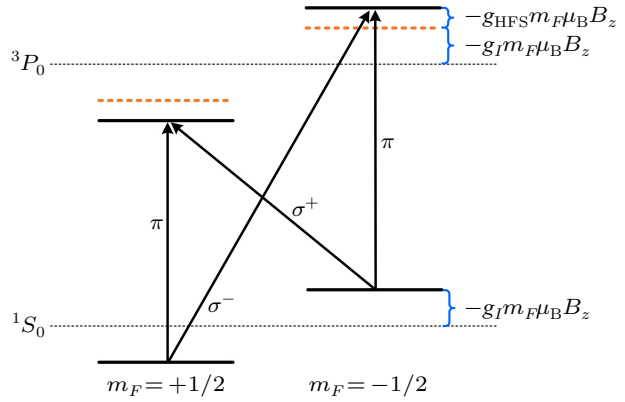


Fig. 2. Zeeman substructure of ^{171}Yb clock transition in a weak magnetic field. The sub-states of $^1S_0$ are affected by the nuclear spin effect only and the energy shift is $-g_I m_F \mu_{\rm B} B_z$, while the $^3P_0$ substates experience nuclear spin effect and hyperfine-induced states mixing with energy shift of $-(g_I + g_{\rm HFS}) m_F \mu_{\rm B} B_z$. The fine dot line represents the energy levels of $^1S_0$ and $^3P_0$ without Zeeman effect. The orange dash line represents the energy levels shift of $^3P_0$ contributed by nuclear spin effect.

Similar to the background magnetic field compensation experiments, we firstly measure the splitting of π transition at a fixed bias magnetic field by self-comparison and the polarization direction of the 578-nm interrogation laser is aligned parallel to the bias magnetic field. Then, the splitting of σ transitions are also recorded at the same bias magnetic field by self-comparison. The experimental conditions are the same as measuring the splitting of two π transitions, except that the polarization direction of the 578 nm is adjusted to be perpendicular to the bias magnetic field. Figures 3(a) and 3(b) show the splitting of π and σ transitions and the splitting ratio η under five different bias magnetic fields, respectively. The measurement time of each point is about thirty minutes. The weighted mean value of η is determined to be 4.759(1) and then the $g_{\rm HFS}$ factor is calculated to be $2.8506(8) \times 10^{-4}$. The first-order Zeeman coefficient of π transitions is further deduced to be $\alpha = -g_{\rm HFS} m_F \mu_{\rm B} = 199.49(5)$ Hz/Gs, in good agreement with NIST group measurement value of 199.516(2) Hz/Gs.[2]

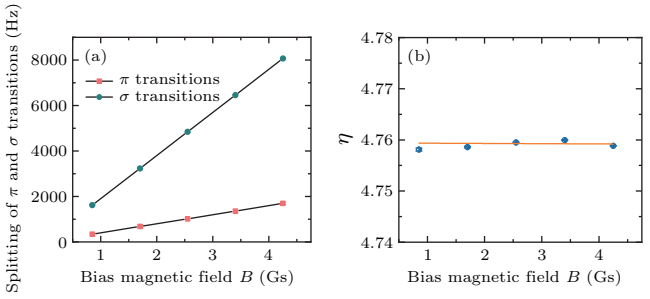


Fig. 3. Evaluation of the first-order Zeeman coefficient of ^{171}Yb clock transition. (a) The splitting of π (cyan circle) and σ (orange square) transitions under five different bias magnetic fields. All data points are connected to guide the eyes. (b) The ratio values of $\eta = (\delta E_B^{\sigma})/(\delta E_B^{\pi}) = 2(g_I/g_{\rm HFS}) + 1$ under five different bias magnetic fields. The orange line represents a weighted mean of five measurements of $\eta = 4.759(1)$. Then we can deduce the first-order Zeeman coefficient of $\alpha = 199.49(5)$ Hz/Gs.

4. Second-order Zeeman coefficient

The second-order Zeeman shift must be taken into account for high accuracy optical clocks. The second-order Zeeman shift uncertainty depends on the uncertainty of both the second-order Zeeman coefficient β and the bias magnetic field $B_{\rm bias}$. The bias magnetic field $B_{\rm bias}$ can be precisely determined by the splitting of π transition and the first-order Zeeman coefficient. Thus, precise measurement of β is critical for evaluating the second-order Zeeman shift. The second-order Zeeman shift of ^{171}Yb clock transition is dominated by the interaction of the $^3P_0$ and $^3P_1$ states and the shift can be approximated as[21,23]

$$\delta f_B^{(2)} \cong -\frac{2\mu_{\rm B}^2}{3(\Delta\nu_{10})h^2} B^2 = \beta B^2, \tag{4}$$

where $h\Delta\nu_{10}$ is the energy separation of $^3P_0$ and $^3P_1$ states. β obtained by theoretical calculation is -6.2 Hz/mT^2.[24]

In order to measure β, we present a self-comparison measurement by monitoring the clock frequency shift between high- and low-bias magnetic fields. The modulation of bias magnetic field is achieved by changing the bias coils currents. Unlike the case of measuring the first-order Zeeman coefficient in the above, two interleaved servo loops are both locked to the center of two π transitions. In the experiment, we fix the low-bias reference magnetic field as $B_0 = 1.7$ Gs, while modulate high-bias magnetic fields B_1 from 0.85 Gs to 4.3 Gs. Each measurement time is about four hours. Figure 4(a) shows a typical instability of interleaved measurement, which can be fitted by a white frequency noise asymptote of $9.5 \times 10^{-16}/\sqrt{\tau}$, and reaches 10^{-18} level over 9000-s averaging time. Then, we calculate the clock frequency differences under different high-bias magnetic fields which are shown in Fig. 4(b). The data are fitted with a linear function of $\Delta f = f_{\rm H} - f_{\rm L} = \beta(B_1^2 - B_0^2)$, where $f_{\rm H}$ and $f_{\rm L}$ are the frequency corrections of high and low bias magnetic fields, respectively. The second-order Zeeman coefficient is determined to be $\beta =$

$-6.09(3)$ Hz/mT^2. The result is in good agreement with NIST group measurement values of $-6.095(7)$ Hz/mT^2,[2] and is compared with previous measurements by other groups in Fig. 4(c).

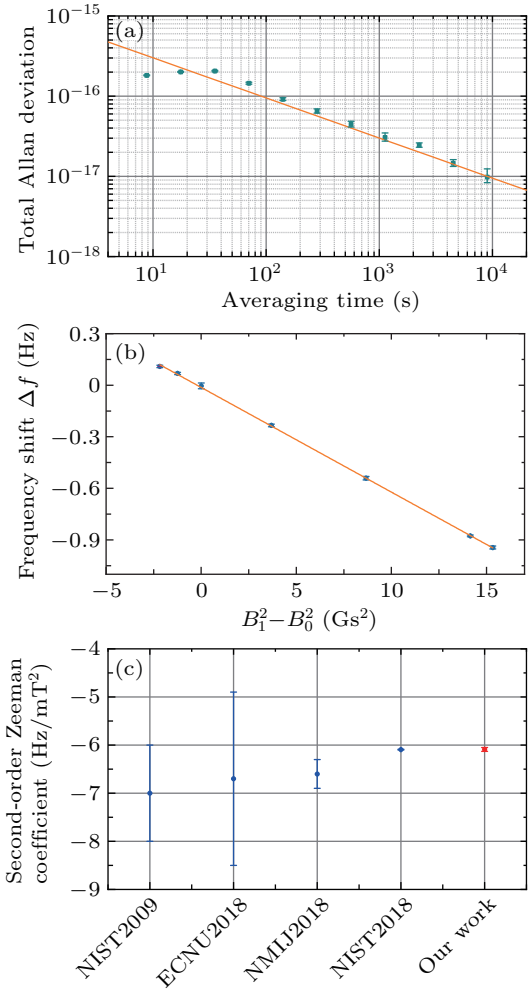


Fig. 4. Evaluation of the second-order Zeeman coefficient of ^{171}Yb clock transition. (a) The instability evaluation of interleaved measurements for the second-order Zeeman shift measurement. The solid line represents the white frequency noise asymptote of $9.5\times10^{-16}/\sqrt{\tau}$, where τ is averaging time in seconds. Error bars are 1σ uncertainty. (b) The relationship between the frequency differences Δf and $(B_1^2-B_0^2)$. The second-order Zeeman coefficient is found to be $\beta=-6.09(3)$ Hz/mT^2 by linear fitting (orange line). Error bars represent 1σ standard deviation obtained from the last point of the total Allan deviation of self-comparison. (c) A history of evaluations of the second-order Zeeman coefficient completed by the NIST,[2,25] ECNU,[26] NMIJ.[27]

5. Vector Stark shift

The m_F-dependent Stark shift induced by lattice laser can also lead to energy shift of the magnetic sublevels, including vector and tensor Stark shift. For ^{171}Yb, the tensor Stark shift is zero due to the angular momentum of $F=1/2$.[28] The vector Stark shift can be written as

$$\Delta f_{\text{vector}}=-\alpha^{\text{V}}\frac{m_F}{2F}\xi\frac{E^2}{2h}, \tag{5}$$

where α^{V} is the vector polarizability, ξ is the degree of ellipticity of the lattice laser and E^2 represents its intensity. For pure circular (linear) polarization, $\xi=\pm1$ ($\xi=0$). Because the vector Stark shift behaves like a pseudomagnetic field along the light propagation axis, it can also cause splitting of π transitions like the magnetic field. The vector Stark shift can be canceled by averaged interrogation for equal but opposite m_F magnetic sublevels, but it will degrade the measurement accuracy of B_{bias} and the evaluation of the second-order Zeeman shift. We have already applied a high-quality Glan–Taylor polarizer (extinction ratio $>10^5$) for lattice laser before entering the science chamber, which would in principle eliminate the vector Stark shift. However, the birefringence of the vacuum windows can deteriorate the polarization purity of lattice laser, and induces a nonzero vector Stark shift. According to Eq. (5), the vector Stark shift and lattice trap depth are linearly related. Therefore, we can measure the frequency difference of the splitting of π transitions at high and low trap depth by self-comparison to extract the vector Stark shift.

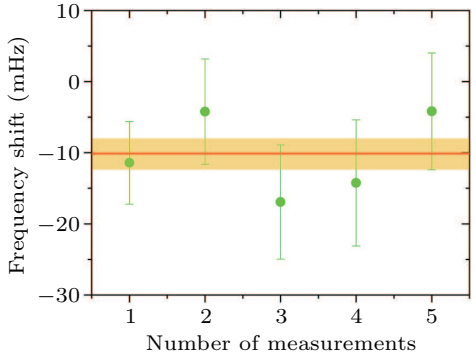


Fig. 5. Five measurements of the vector Stark shift for $0.26U_0$ variation. Green filled circles are each measured value and error bars are standard errors. The red line represents the weighted mean and the orange shaded region represents the statistical 1σ standard deviation of the five measurements. For $0.26U_0$ trap depth variation, $\delta f_{\text{vector}}=-10.1(2)$ mHz.

In normal clock operation, the lattice trap depth $U_0=200E_{\text{r}}$ is extracted from sideband spectrum, where E_{r} is lattice photon recoil energy. We modulate trap depth between $0.74U_0$ and U_0 in two interleaved servo loops and measure the frequency difference at two trap depths. We repeat this measurement for five times and each measurement time is about four hours. Figure 5 shows that the difference of vector Stark shift at two different trap depth is $-10.1(2)$ mHz. Then we deduce the vector Stark shift of $-39(9)$ mHz for normal clock operation with trap depth of U_0. We have removed the vector Stark shift in the first- and second-order Zeeman coefficient measurements in the above.

6. Conclusion

In this paper, we presented a precise measurement of magnetic constants of ^{171}Yb clock transition based on our new optical clock. For normal clock operation, we compensate the background magnetic field to <1 mGs. The first-order Zeeman coefficient of π transitions is determined to be $\alpha=199.49(5)$ Hz/Gs by measuring the splitting ratio of π

and σ transitions. By self-comparison, the second-order Zeeman coefficient is measured to be $\beta = -6.09(3)$ Hz/mT^2 and the vector Stark shift is $-39(9)$ mHz for our ^{171}Yb optical lattice clock. We extrapolate the second-order Zeeman shift to be $\Delta\nu/\nu = (-340 \pm 1.8) \times 10^{-18}$ at 1.7-Gs bias magnetic fields for our ^{171}Yb optical lattice clock. For a normal bias magnetic field of 1 Gs, the second-order Zeeman shift uncertainty can be reduced to 10^{-19} level.

Acknowledgments

Project supported by the National Key Research and Development Program of China (Grant No. 2017YFA0304402), the National Natural Science Foundation of China (Grant Nos. U20A2075 and 11803072), and the Strategic Priority Research Program of the Chinese Academy of Sciences (Grant No. XDB21030100).

References

[1] Schioppo M, Brown R C, McGrew W F, Hinkley N, Fasano R J, Beloy K, Yoon T H, Milani G, Nicolodi D, Sherman J A, Phillips N B, Oates C W and Ludlow A D 2017 *Nat. Photon.* **11** 48
[2] McGrew W F, Zhang X, Fasano R J, Schaffer S A, Beloy K, Nicolodi D, Brown R C, Hinkley N, Milani G, Schioppo M, Yoon T H and Ludlow A D 2018 *Nature* **564** 87
[3] Bothwell T, Kedar D, Oelker E, Robinson J M, Bromley S L, Tew W L, Ye J and Kennedy C J 2019 *Metrologia* **56** 065004
[4] Oelker E, Hutson R B, Kennedy C J, Sonderhouse L, Bothwell T, Goban A, Kedar D, Sanner C, Robinson J M, Marti G E, Matei D G, Legero T, Giunta M, Holzwarth R, Riehle F, Sterr U and Ye J 2019 *Nat. Photon.* **13** 714
[5] Huntemann N, Sanner C, Lipphardt B, Tamm C and Peik E 2016 *Phys. Rev. Lett.* **116** 063001
[6] Huang Y, Zhang B, Zeng M, Hao Y, Ma Z, Zhang H, Guan H, Chen Z, Wang M and Gao K 2022 *Phys. Rev. Appl.* **17** 034041
[7] Nicholson T L, Campbell S L, Hutson R B, Marti G E, Bloom B J, McNally R L, Zhang W, Barrett M D, Safronova M S, Strouse G F, Tew W L and Ye J 2015 *Nat. Commun.* **6** 6896
[8] Ushijima I, Takamoto M, Das M, Ohkubo T and Katori H 2015 *Nat. Photon.* **9** 185
[9] Brewer S, Chen J, Hankin A, Clements E, Chou C, Wineland D, Hume D and Leibrandt D 2019 *Phys. Rev. Lett.* **123** 033201
[10] Lodewyck J, Bilicki S, Bookjans E, Robyr J L, Shi C, Vallet G, Le Targat R, Nicolodi D, Le Coq Y, Guéna J, Abgrall M, Rosenbusch P and Bize S 2016 *Metrologia* **53** 1123
[11] Riehle F, Gill P, Arias F and Robertsson L 2018 *Metrologia* **55** 188
[12] Takamoto M, Ushijima I, Ohmae N, Yahagi T, Kokado K, Shinkai H and Katori H 2020 *Nat. Photon.* **14** 441
[13] Bothwell T, Kennedy C J, Aeppli A, Kedar D, Robinson J M, Oelker E, Staron A and Ye J 2022 *Nature* **602** 420
[14] Zheng X, Dolde J, Lochab V, Merriman B N, Li H and Kolkowitz S 2022 *Nature* **602** 425
[15] Kolkowitz S, Pikovski I, Langellier N, Lukin M D, Walsworth R L and Ye J 2016 *Phys. Rev. D* **94** 124043
[16] Kennedy C J, Oelker E, Robinson J M, Bothwell T, Kedar D, Milner W R, Marti G E, Derevianko A and Ye J 2020 *Phys. Rev. Lett.* **125** 201302
[17] Liu H, Zhang X, Jiang K, Wang J, Zhu Q, ZXXiong, He L and Lyu B 2017 *Chin. Phys. Lett.* **34** 020601
[18] Xiong D, Zhu Q, Wang J, Zhang A, Tian C, Wang B, He L, Xiong Z and Lyu B 2021 *Metrologia* **58** 035005
[19] Zhang A, Xiong Z, Chen X, Jiang Y, Wang J, Tian C, Zhu Q, Wang B, Xiong D, He L, Ma L and Lyu B 2022 *Metrologia* **59** 065009
[20] Lemke N D 2012 *Optical lattice clock with spin-1/2 ytterbium atoms*, Ph. D. Dissertation (University of Colorado at Boulder) p. 57
[21] Boyd M M, Zelevinsky T, Ludlow A D, Blatt S, Zanon-Willette T, Foreman S M and Ye J 2007 *Phys. Rev. A* **76** 022510
[22] Olschewski L and Otten E W 1967 *Zeitschrift für Physik* **200** 224
[23] Ludlow A D, Boyd M M, Ye J, Peik E and Schmidt P 2015 *Rev. Mod. Phys.* **87** 637
[24] Taichenachev A V, Yudin V I, Oates C W, Hoyt C W, Barber Z W and Hollberg L 2006 *Phys. Rev. Lett.* **96** 083001
[25] Lemke N D, Ludlow A D, Barber Z W, Fortier T M, Diddams S A, Jiang Y, Jefferts S R, Heavner T P, Parker T E and Oates C W 2009 *Phys. Rev. Lett.* **103** 063001
[26] Gao Q, Zhou M, Han C, Li S, Zhang S, Yao Y, Li B, Qiao H, Ai D, Lou G, Zhang M, Jiang Y, Bi Z, Ma L and Xu X 2018 *Sci. Rep.* **8** 8022
[27] Kobayashi T, Akamatsu D, Hisai Y, Tanabe T, Inaba H, Suzuyama T, Hong F L, Hosaka K and Yasuda M 2018 *IEEE Trans. Ultrason. Ferroelectr. Freq. Control* **65** 2449
[28] Angel J R P and Sandars P G H 1968 *Proc. R. Soc. A* **305** 125